Study on the Pyrolysis Characteristic and the Microstructure of the Pyrolysis Products of β Resins from Different Coal Tar Pitch

[1]Yaming Zhu, [1]Xuefei Zhao*, [1]Lijuan Gao, [1,2]Jun Lv, [1]Junxia Cheng, [1]Shiquan Lai
[1]*Engineering research center of advanced coal coking and efficient use of coal resources, University of Science and Technology Liaoning, Anshan 114051, Liaoning, China.*
[2]*College of chemistry and chemical engineering, Qiqihar University, Qiqihar 161006，Heilongjiang, China.*
zhao_xuefei@163.com*

(Received on 27th February 2017, accepted in revised form 15th February 2017)

Summary: Three types of β resins, namely, β-1, β-2, and β-3 were obtained from a medium coal tar pitch, modified pitch A, and modified pitch B, respectively. The pyrolysis characteristics of these three β resins were studied by TG/DTG analysis, FTIR spectroscopy, and curve-fitting method. The pyrolysis of β-1 showed a two-step mass loss, and the pyrolysis of β-2 showed a one-step mass loss. However, the pyrolysis of β-3 showed a three-step mass loss. This difference in pyrolysis among the three β resins was caused by the dissimilarity in their aromaticity index (Iar) and CH_3/CH_2 ratio; these factors significantly affect the aromaticity and number of aliphatic side chains in β resin. The polarized microscopic structures of the pyrolysis products β-1-P, β-2-P, and β-3-P obtained from β resins show that β-1-P mainly has a coarse fibrous structure, whereas β-2-P and β-3-P have a mosaic structure and fine fibrous structure, respectively. The results of XRD and Raman analysis combined with curve-fitting method show that the content of ordered carbon microcrystalline structure in β-3-P is higher than the contents of other two samples, and β-2-P has the lowest content of this microcrystalline structure. In fact, the lower Iar (<0.5) corresponded to a mosaic structure, and the higher Iar (>0.8) corresponded to a fibrous structure. Moreover, oxidation linking reaction inhibited the formation of plane macromolecules, thus hindering the formation of an optically anisotropic fibrous structure during the pyrolysis of coal tar pitch.

Keywords: Coal tar pitch, β resins, Pyrolysis characteristic, Microscopic structure, Quantity analysis.

Introduction

International Union of Pure and Applied Chemistry (IUPAC) define pitch as a solid material at room temperature, i.e., the residue obtained after the pyrolysis of organic materials or distillation of tar [1]. Coal tar pitch is a black, sticky solid material with a very high viscosity [2]. This also indicates that coal tar pitch is a complex material consisting of aromatic compounds with a broad molecular weight distribution [3]. Coal tar pitch is a promising candidate to produce carbon materials and carbon/carbon composites owing to its low cost and high performance to generate graphitizable carbons [4–6].

To obtain carbon materials or carbon/carbon composites with coal tar pitch as the matrix precursor, it is necessary to perform the deep processing of coal tar pitch [7, 8]. In previous studies [9–14], thermal treatment and air oxidation are the most common methods for the modification of coal tar pitch. These treatments cause the polymerization and condensation of pitch components, increasing their molecular weight [13]. Pitches show different compositions depending on the treatment [15]. The characterization of a modified pitch is fundamental to better understand their functional properties according to the experimental conditions. Thermal analyses (TG, DTG, and DTA) are useful to characterize pitches as they easily distinguish pitches of different origins or allocated for different uses, or even distinguish pitches of the same origin, but prepared following different procedures [16, 17]. Fourier transforms infrared (FTIR) spectroscopy and curve-fitting methods are helpful to determine the pitch aromaticity and identify functional groups and aliphatic and aromatic hydrogens [18–24].

β resin is a component of toluene insoluble and quinoline soluble (TI-QS) part of coal tar pitch. β resin has a narrow distribution of molecular weight, good fluidity, and good caking properties. All these properties endow β resin with a good reactivity and broad reaction temperature. In fact, the content of β resin is a prerequisite to determine the feasibility of coal tar pitch to produce high-quality carbon/graphite materials. The content of β resin plays a key role in the coal tar pitch processing phases [25, 26]. The property of β resin significantly affects the thermal treatment and air oxidation of coal tar pitch. The purpose of this study is to compare the pyrolysis behaviors and characteristics of β resins obtained from a medium coal tar pitch and modified pitches

*To whom all correspondence should be addressed.

obtained by thermal treatment and air oxidation by TG/DTG analysis, FTIR spectroscopy, and curve-fitting method. In addition, the microstructural characteristics of pyrolysis products obtained from β resins were successfully evaluated by various analysis methods.

Experimental

Materials

The medium coal tar pitch was purchased from Shanxi Coking Plant (Shanxi, China). Toluene and quinoline were purchased from Tianjin Regent Chemicals (Tianjin, China). The proximate analysis of medium coal tar pitch is shown in Table-1.

Preparation of modified pitch

A refined pitch prepared from the medium pitch was used as the raw material for preparing the modified pitchs. Modified pitch A was obtained by air oxidation in a stainless steel reactor. The refined pitch was heated to 280 °C at a heating rate of 5 °C/min, the holding time was 6 h, and air was used as the oxygen supply agent. Thermal treatment was used to prepare modified pitch B. Briefly, 100 g of refined pitch was heated to 420 °C at a heating rate of 5 °C/min, the holding time was 4 h, and N_2 was used as the protection gas. The proximate analysis of refined pitch and modified pitches is shown in Table-1.

Table-1: Proximate Analysis of pitch Samples.

Sample	SP[a] /°C	TI[b] /wt%	QI[c] /wt%	CV[d] /wt%	β resin[e] /wt%
Medium pitch	**73**	**19.65**	**5.32**	**49.15**	**14.33**
Refined pitch	**49**	**10.95**	**0.07**	**41.76**	**10.88**
Modified pitch A	**232**	**53.16**	**30.18**	**52.33**	**22.98**
Modified pitch B	**228**	**60.29**	**25.39**	**81.88**	**34.90**

[a] Softening point, [b] Toluene insoluble, [c] Quinoline insoluble, [d] Coke value, [e] TI-QS

Preparation of β resins

Three types of β resins, namely, β-1, β-2 and β-3 were obtained from the medium coal tar pitch, modified pitch A and modified pitch B. The β resin was obtained using a two-step solvent extraction method at 90 °C. In the first step, the toluene-insoluble part (TI) in the coal tar pitch was obtained using toluene as the solvent. Briefly, 30 g of coal tar pitch and 600 mL of toluene as the solvent were charged into a three-neck flask, and the coal tar pitch was extracted for 3 h under stirring at 90 °C. The mixture was filtered, and the residue was TI. In the second step, the quinoline-soluble part (QS) in the TI was obtained using quinoline as the solvent. The extraction and filtration processes were the same as above. The filtrate was distillated at 240 °C. The distillation residue was β resin.

Characterization of β resins

Ultimate analysis of β resins

The ultimate analysis of β resins was performed using a Vario EL β elemental analyzer (Elementar, Germany). Oxygen content was calculated using the difference method. Table-2 shows the ultimate analysis data of β resins.

Table-2: Ultimate analysis of β resins.

Samples	C/%	H/%	N/%	S/%	O/%	C/H
β-1	**92.22**	**3.78**	**1.25**	**0.48**	**2.27**	**2.03**
β-2	**91.95**	**3.81**	**1.22**	**0.38**	**2.64**	**2.01**
β-3	**93.05**	**3.93**	**1.20**	**0.37**	**1.45**	**1.97**

Thermogravimetric analysis (TGA)

TGA and derivative thermogravimetry (DTG) measurements (TAQ500, USA) were carried out under a N_2 flow rate of 100 mL min^{-1}, the samples mass was 10 mg, the temperature ranged from 20 °C to 650 °C, and the heating rate was 10 °C min^{-1}. Fig 3 shows the TG/DTG analysis of β resins.

FTIR spectroscopy

The FTIR spectra of β resins were obtained using a NICOLETIS5 FT-IR spectrometer at a resolution of 4 cm^{-1}. Prior to the FTIR analysis, KBr pellets were prepared by grinding a mixture of 1 mg of sample with 150 mg of KBr. Duplicate pellets were used for the quantitative measurements. The aliphatic (Hal) contents were calculated from the integrated absorbance areas of the bands at 3000–2700 cm^{-1}. The bands in the IR spectra were assigned according to the literature [27, 28].

Characterization of pyrolysis products

Polarizing microscope analysis

A polarizing microscope (Axio Scope A1 pol, Carl Zeiss, Germany) was used to characterize the optical microstructure of samples. Briefly, the pyrolysis products of β resin (β-1-P, β-2-P, and β-3-P) obtained at 650 °C was embedded in epoxy resin, and the micro-object was obtained by sanding and polishing. Then, the sample was placed under a microscope with

two drops of cedar oil. The graphs of samples obtained from the polarizing microscope are shown in Fig. 4.

XRD analysis

β-1-P, β-2-P, and β-3-P were characterized by powder X-ray diffraction (XRD) analysis with a tube voltage of 40 kV, tube current of 40 mA, scanning range of 10–90°, and step size of 0.013°.

Raman spectroscopic analysis

The carbon microcrystalline structures of β-1-P, β-2-P, and β-3-P were determined by Raman spectroscopy (LabRAM HR Evolution, JOBIN YVON, France) with an incident wavelength of 532 nm. The distribution and contents of carbon microcrystalline structures were calculated from the integrated intensity areas of the bands at 900–1800 cm^{-1}. The bands in the Raman spectra were assigned according to the literature [29–32], as shown in Table-4. Briefly, D3 band was fitted by a Gaussian function, but the other four bands were fitted by a Lorenz function.

Curve-fitting analysis

Selected zones of the FTIR and Raman spectra were studied by curve-fitting analysis using a commercially available data-processing program (Origin 7.0). Prior to the curve-fitting analysis, background corrections were applied as described in the literature [27, 28, 33]. The initial approximation of the number of bands and peak positions was obtained by determining the second derivatives of the spectral data, and Gaussian and Lorentz functions were used as the mathematical functions [34].

To determine the goodness of fit criteria, the following aspects were considered: coefficient of determination (COD) and standard errors of parameters (chi-squared). Briefly, all the COD values of the curve-fitting analysis in all the cases were above 0.999, and the chi-squared was $<10^{-5}$.

Results and discussion

Qualitative and quantitative FTIR analysis of β resins

FTIR Spectroscopy is one of the most common techniques to achieve information about functional groups in complex solids. This has also been used as an effective tool for the quantitative estimation of structures of pitches combined with the curve-fitting method. Fig. 1 shows the FTIR spectra of β resins obtained from different coal tar pitches. The peak at 3050 cm^{-1} can be attributed to the aromatic stretching mode, and the peaks between 3000—2700 cm^{-1} can be attributed to the aliphatic C–H stretching mode. Peaks in the region 900–700 cm^{-1} can be attributed to the aromatic C–H out-of-plane bending mode.

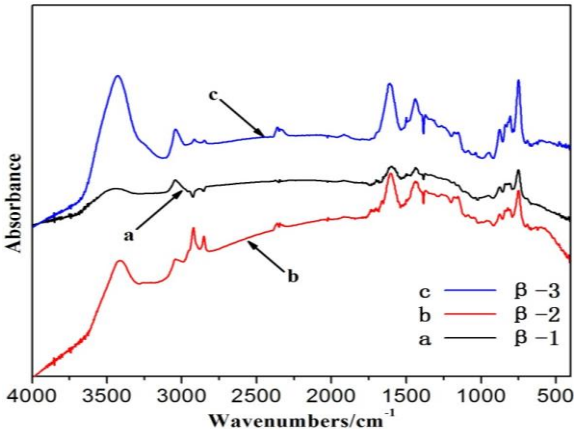

Fig. 1: FTIR spectra of β resins.

To further evaluate the imparity of β resins from different coal tar pitches, the 3000—2800 cm^{-1} was studied by curve-fitting analysis. A series of relationships defined as the ratios of integrated absorbance areas were used to quantify the structural changes from the curve-fitting bands. Iar is the aromatic hydrogen index, and CH_3/CH_2 ratio is the aliphatic side chain index, obtained from the ratios of integrated absorbance peak areas. For example, Abs ·3050 is the integration area of absorbance in 3050 cm^{-1} fitting peak. The relationships can be expressed as follows:

Table-3: Raman bands and vibration modes reported by literatures [29-32].

Band	Raman shift (cm^{-1})	Vibration mode
G	1580	Ideal graphitic lattice (E_{2g}-symmetry)
D1	1350	Disordered graphitic lattice (graphene layer edges, A_{1g} symmetry)
D2	1620	Disordered graphitic lattice (surface graphene layers, E_{2g}-symmetry)
D3	1500	Amorphous carbon (Gaussion line shape)
D4	1200	Disordered graphitic lattice (A_{1g} symmetry), polyenes , ionic impurities

$$Iar = Abs \cdot 3050/(Abs \cdot 3050 + Abs \cdot 2920) \quad (1)$$

$$CH_3/CH_2 = 2950\ cm^{-1}\ band/2920\ cm^{-1}\ band \quad (2)$$

Equation 1 shows the aromaticity of β resin. Equation 2 shows the ratio of methyl/methylene structures, and it can be considered as an estimate of the length of aliphatic chains of β resin [22, 34].

Table-3 shows the aromaticity index of β resins. A clear difference was observed among the three β resins. The aromaticity index of β-1 and β-3 were both >0.85, indicating that these two β resins have a high aromaticity. However, the aromaticity index of β-2 was <0.5. This indicates that β-2 has a lower aromaticity, but a higher content of aliphatic hydrogen. The data shown in Table-4 also indicate that the integration area of aliphatic C–H stretching mode in β-2 resin was five times higher than those of the other two β resins.

Table-4: The index of Iar on β resins.

Samples	Centre/cm^{-1}	Height[1]	Width/cm^{-1}	Area[2]	Iar
β-1	3043	0.01616	64.604	1.12021	0.85
	2925	0.00908	20.249	0.19756	
β-2	3044	0.01362	48.212	0.66933	0.46
	2921	0.03028	22.178	0.78575	
β-3	3043	0.03033	53.033	1.64343	0.91
	2918	0.00584	24.106	0.16129	

[1]Absorbance，[2]Integrate absorbance unit ×cm^{-1}

To better understand the distribution of aliphatic hydrogen and number of alkyl chains in β resins, the curve-fitting analysis of 3000–2700 cm^{-1} was carried out. The aliphatic region of raw coal tar pitch can be curve-fitted to a series of five bands attributed to asymmetric −CH_3 and −CH_2− stretching (2953 and 2923 cm^{-1}, respectively), symmetric −CH_3 and −CH_2− stretching (2879 and 2853 cm^{-1}, respectively), and methine C−H stretching (2896 cm^{-1}), as shown in Fig. 2. The results are shown in Table-5.

Table-5: Curve-Fitting for the Aliphatic C-H Stretching Bands of β Resin from Different Pitches.

Centre(cm^{-1})	Assignment	Width(cm^{-1})			Height[1]			Area[2]		
		β-1	β-2	β-3	β-1	β-2	β-3	β-1	β-2	β-3
2853	Sym. R_2CH_2	27.524	25.596	28.919	0.005	0.015	0.003	0.087	0.220	0.053
2870	Sym. RCH_3	33.091	67.454	83.767	0.002	0.009	0.002	0.039	0.338	0.102
2896	R_3CH	79.138	55.759	59.571	0.003	0.013	0.003	0.138	0.433	0.100
2923	Asym. R_2CH_2	39.147	39.502	41.519	0.011	0.034	0.006	0.250	0.780	0.151
2953	Asym. RCH_3	52.875	57.035	41.519	0.004	0.012	0.001	0.138	0.398	0.028

[1]Absorbanc, [2]Integrate absorbance unit×cm^{-1}

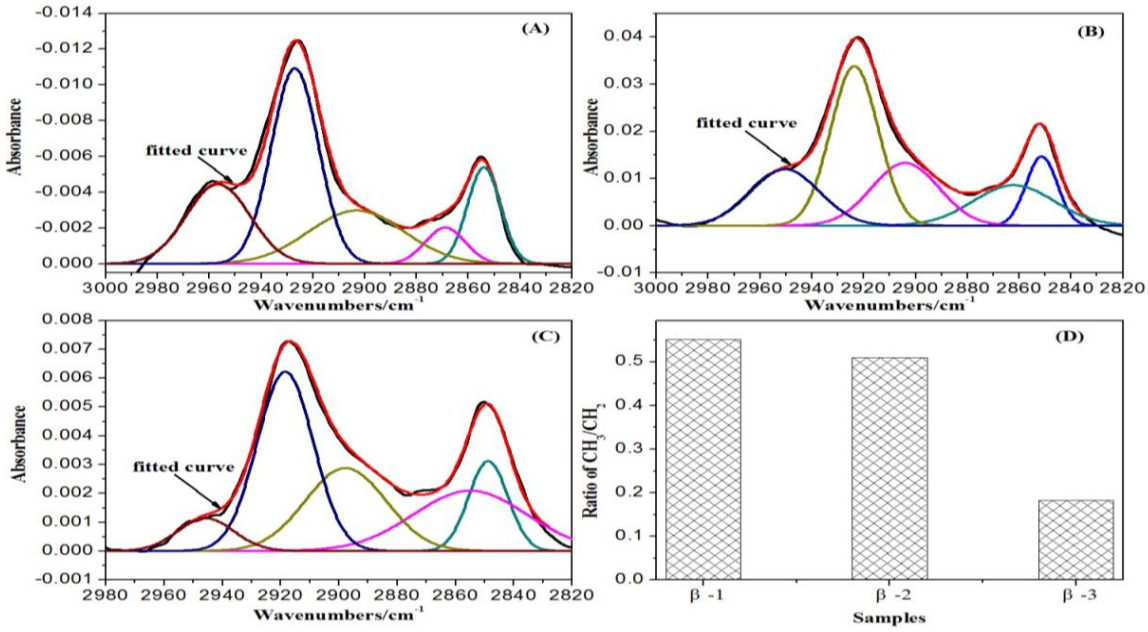

Fig. 2: Curve-fitted IR spectrum of the aliphatic C-H stretching bands for β resin from different pitches: (A) β-1，（B）β-2, （C）β-3, (D) The ratio of CH_3/CH_2 of samples.

According to the literature [34], the CH_3/CH_2 ratio reflects the length of aliphatic chain and branched chain. The changes in the aliphatic bands of three β resins (CH_3/CH_2 ratio shown in Fig. 2 (D)) indicate that the ratio of β-3 resin is significantly lower than other two β resins. This shows that the length of aliphatic chain of β-3 is longer, and the length of aliphatic branched chains is also longer.

Compared to β-1 and β-2, β-3 has the highest aromaticity and most aliphatic chain [Table-4 and Fig. 2 (D)]. This is probably caused by the high condensation degree in β-3. Air oxidation destroyed the aromatic C=C bonds, while hindering the growth of aliphatic chains [Fig. 2 (D)]. Therefore, β-2 extracted from modified pitch A has the lowest Iar (Table-4).

TGA

Thermal analysis methods are the most promising methods to study the pyrolysis behavior of pitches and characterize them. Thermal analysis methods are efficient to evaluate the nature of the reaction. TGA provides information about the mass loss associated with reactions. TGA and DTG also provide information about mass loss and the rate of mass loss at a particular temperature.

Initially, the pyrolysis of β-1, β-2, and β-3 was carried out by TGA to study the different pyrolysis characteristics of β resins obtained from different pitches. The TGA and DTG curves (Fig. 3) show a significant difference in the pyrolysis characteristics of β resins.

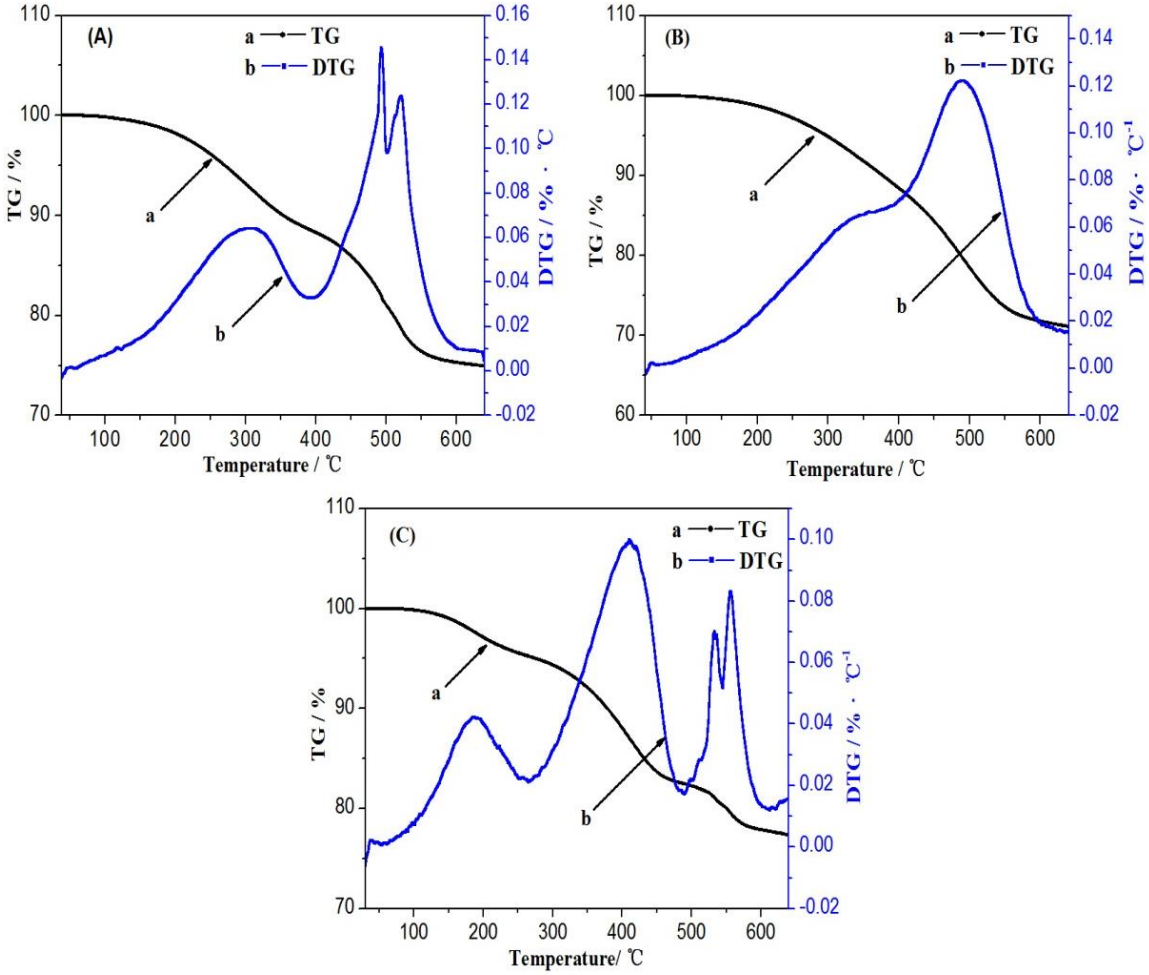

Fig. 3: TG/DTG analysis of β resins：(A) β-1, (B) β-2, (C) β-3.

The TG and DTG curves (Fig. 3 A) show that β-1 mass loss clearly occurs in two separate steps. In the first step (180–400 °C), β-1 loses 11.78 wt% of mass, and the temperature of maximum mass loss (T_{max}) was 285 °C. In the second step (450–600 °C), the T_{max} is 493 °C. This indicates that β-1 contains two different components of different thermal stabilities and compositions. In fact, the elemental analysis shows that the total carbon, oxygen, and hydrogen contents account for 98.27 wt% of the total content (Table-2), the other components being sulfur and nitrogen. On the other hand, the FTIR spectra (Figs. 1 and 2), Iar index (Table-4), and CH_3/CH_2 ratio (Fig. 2D) show that β-1 contains mainly an aromatic ring structure and secondly aliphatic side chains. In other words, the molecular structure of β-1 was composed of a large number of polycyclic aromatic molecules with some aliphatic side chains. When the temperature was increased to 180–400 °C, the aliphatic side chains began to fracture, and the fist step of mass loss occurred with the escape of small molecules of poor thermal stability. Molecules with a higher thermal stability escaped as the temperature was increased to 450–600 °C.

Fig. 3 B shows that β-2 mass loss is completed in a single step in a wide temperature range 200–600 °C. The carbonaceous residue is 68.75 wt% at 800 °C, and the T_{max} is 493 °C. The Iar index (Table-4), curve-fitted IR spectrum and data at the zone 3000–2800 cm^{-1} (Fig. 2 B and Table-5), CH_3/CH_2 ratio (Fig. 2D) indicate that β-2 was composed of mainly aliphatic side chains and secondly aromatic ring structures. This is because of the characteristics of modified pitch A, which was obtained by air oxidation. In the presence of oxygen, the aromatic structure of coal tar pitch was destroyed; therefore, the CV content also decreased (Table-1). This also narrowed the molecular distribution. Because of these structural features, the pyrolysis of β-2 showed a single weight-loss peak with a wide weight-loss temperature range.

β-3 weight loss was completed in three separate steps. In the first step (150–250 °C), β-3 lost 5 wt% of the total weight, and the T_{max} was 220 °C. In the second step (260–480 °C), the weight loss was completed, and the T_{max} was 419 °C. In the third step (490–600 °C), the weight loss occurred in a narrow temperature range, and the T_{max} was 556 °C. Compared to β-1 and β-2, the ratio of C/H on β-3 clearly decreased (Table-2). Additional information was obtained by calculation using the FTIR spectra (Fig. 1) combined with curve-fitting at the zone of aliphatic C–H stretching bands for β-3 (Fig. 2 C). The curve-fitting data are shown in Table-5. The Iar index (Table-4) and CH_3/CH_2 ratio (Fig. 2D) show that β-3 has a structure with a high aromaticity index and more aliphatic side chains. These results indicate a cross-linked macromolecular structure in β-3 that occurred in the modification of modified pitch B. During the pyrolysis, the cross-linked bonds were destroyed at a lower temperature. This resulted in residues made up of two components of different thermal stabilities. With persistent overheating, the pyrolysis of two components occurs at different temperature ranges.

Polarized microscopic structure analysis of pyrolysis products

The polarized microscopic images of pyrolysis products obtained from β resins showed significant differences (Fig. 4). Figs. 4 (A) and (B) clearly show that β-1-P had mainly a coarse fiber structure. However, the polarized microscopic images of β-2-P and β-3-P showed a mosaic structure and fine fibrous structure, respectively. These are probably related to the aromaticity index (Table-3). Briefly, the lower Iar (<0.5) corresponds to a mosaic structure, and the higher Iar (>0.8) corresponds to a fibrous structure. Another reason for this difference is the source of β resins. In fact, β-2 was obtained from modified pitch A. However, modified pitch A was prepared by air oxidation, and the O2 present in the system caused the oxidation linking reaction. The oxidation linking reaction inhibits the formation of planar macromolecules in modified pitch A. Therefore, the pyrolysis of β-2 could not create an optical anisotropic fibrous structure, but a mosaic structure.

XRD analysis of samples

The microstructures of samples were determined by XRD analyses. The XRD patterns of the samples are shown in Fig. 5 (A). The trends of the XRD patterns of the three samples are similar. However, β-3 has the largest intensity of (002) and the narrowest width of (002). Compared to β-1-P, β-2-P has the maximum width of (002). In fact, compared to β-1-P and β-2-P, β-3-P has the most ordered microcrystalline structure.

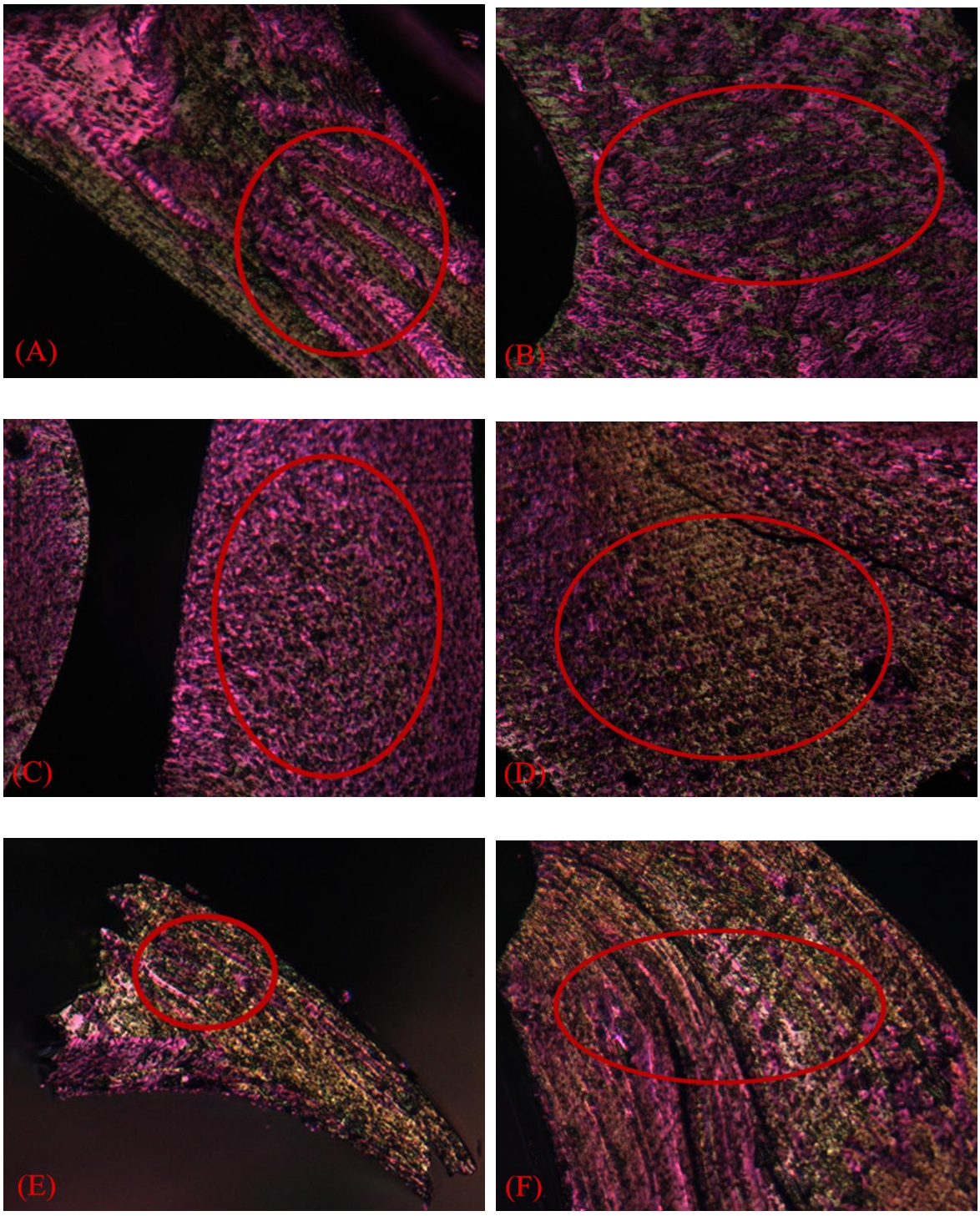

Fig. 4: Polarized microscopic structure analysis of pyrolysis products from β resin, (A) and (B) for β-1-P, (C) and (D) for β-2-P, (E) and (F) for β-3-P.

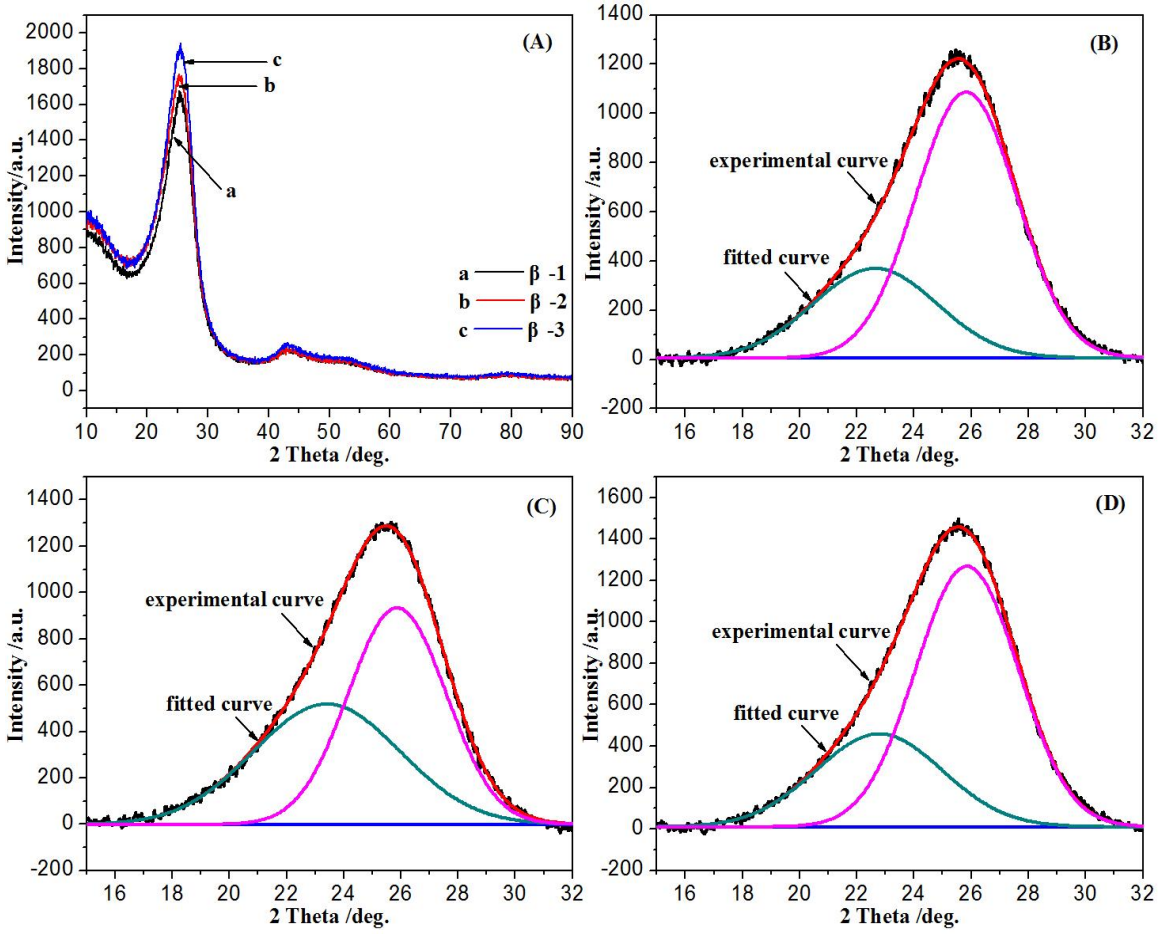

Fig. 5: XRD analyses of samples (A), and curve-fitted graph of pyrolysis product from β resins: (B) for β-1-P, (C) for β-2-P and (D) for β-3-P.

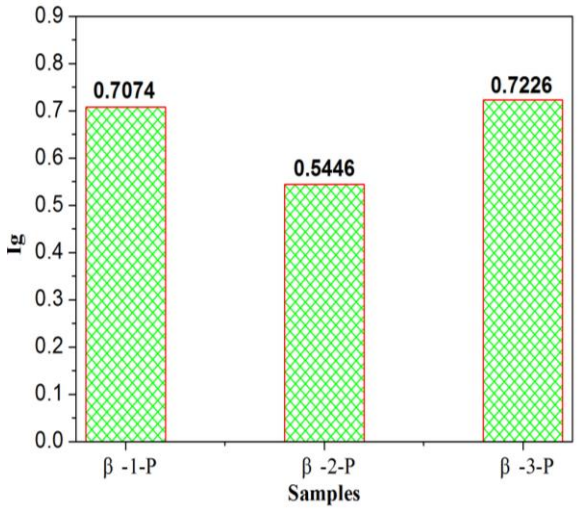

Fig. 6: The distribution of Ig on three samples.

For a better comparison of the microcrystalline structure in the samples, the curve-fitting method has been used. Researchers [35] found that the broad hump of (002) of carbon material can be divided into two Gaussian peaks at 20° and 26° nearby peak-fitting, namely, γ-band and π-band, respectively. The areas of the γ and π peaks are probably equal to the content of amorphous carbon and trended ideal graphite carbon. The content of trended ideal graphite carbon (Ig) can be calculated using the following equation:

$$Ig = A(\pi)/[A(\pi)+A(\gamma)] \quad (3)$$

A(π) and A(γ) are the area of π and γ peaks after the peak-fitting.

The curve-fitting profile of β resins is shown in Figs 5(B), (C), and (D); the distribution of Ig on the samples is shown in Fig. 6. Obviously, the numerical of Ig in β-3-P is higher than β-1-P, and much higher than that in β-2-P. This indicates that the contents of trended ideal graphite carbon of β-3-P and β-1-P were much higher than β-2-P at the same pyrolysis temperature. In other words, the graphitization of β-3-P should be easier than β-2-P. This phenomenon can be explained by the Iar of the samples. A higher aromaticity indicates more planar macromolecules in the molecular components of the sample, easy to graphitize.

Raman spectroscopic analysis of samples

As shown in Fig. 7(A), the two typical bands, the G band (graphite band) and D band (disorder band) were detected in the first-order region in all the studied samples. The Raman spectra obtained from β-1-P and β-3-P showed a higher intensity than β-2-P. To determine the carbon crystalline structure of the samples, the curve-fitting method was used to obtain more information from the Raman spectrum [Figs. 7 (B), (C), and (D)]. The fitting standards are shown in Table-3.

The band area ratios (I_G/I_{All}, I_{D3}/I_G) were used to measure the content of microcrystalline structure in samples (Table-6). β-3-P has the maximum I_G/I_{All} ratio and minimum I_{D3}/I_G ratio. However, these two parameters of β-2-P are contrary to β-3-P. This indicates that the content of well-ordered carbon structure in β-3-P was higher than the other two samples. In contrast, β-2-P has the highest level of amorphous carbon. This phenomenon is identical with the optical microstructure of three samples.

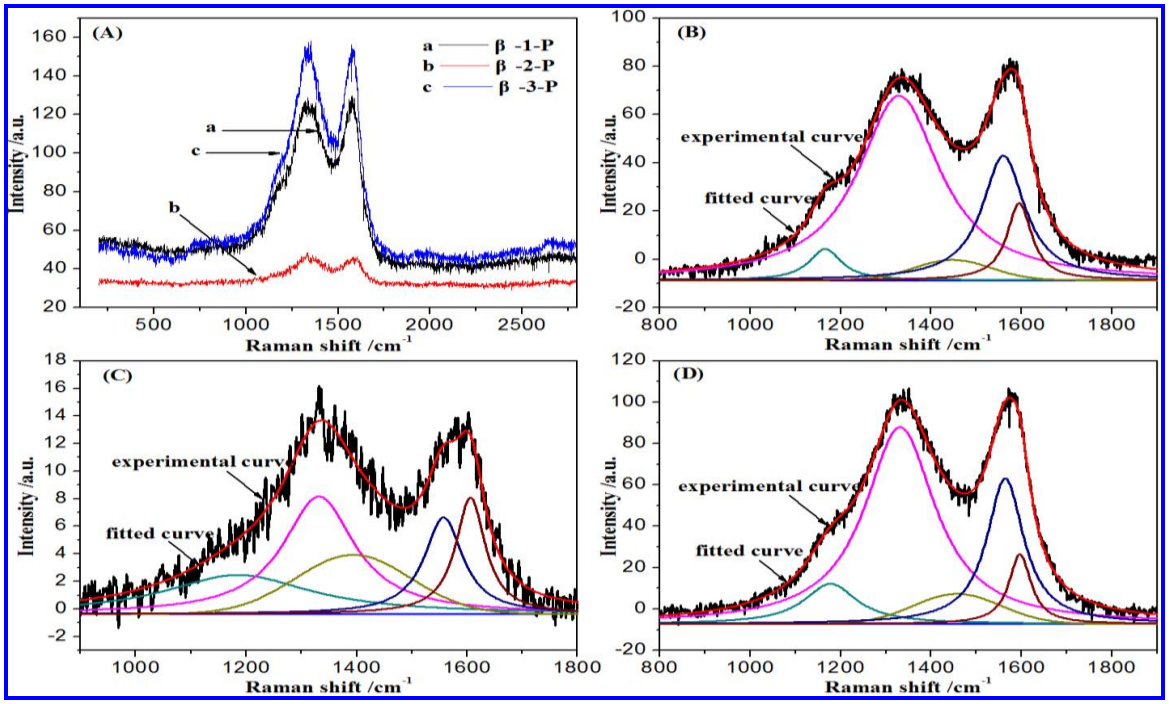

Fig. 7: Raman spectrum analyses of samples (A), and curve-fitted graph of pyrolysis product from β resins: (B) for β-1-P, (C) for β-2-P and (D) for β-3-P.

Table-6: Curve-fitting data of the first-order region for samples.

Samples	Integrate Area					Ratio	
	I_{D1}	I_{D2}	I_{D3}	I_{D4}	I_G	I_G/I_{All}	I_{D3}/I_G
β-1-P	15483.98	2121.44	1202.73	1113.55	5721.16	0.22	0.21
β-2-P	1280.43	552.96	746.98	766.19	587.76	0.15	1.27
β-3-P	16533.92	1905.86	1360.39	2644.46	6838.28	0.23	0.19

Conclusions

The pyrolysis characteristics of different β resins obtained from different coal tar pitchs were evaluated experimentally. Modification methods play a key role on the molecular structure of β resins. FTIR spectroscopic analysis combined with the curve-fitting method showed that the Iar and CH_3/CH_2 ratio of β resins have significant differences. This indicates that β-1 was mainly composed of an aromatic ring structure and secondly aliphatic side chains. β-2 was mainly composed of aliphatic side chains and secondly aromatic ring structures, and β-3 has a high aromaticity index and more aliphatic side chains. These compositions of molecular structure contribute to the two clear weight-loss steps for β-1, a single weight-loss step for β-2, but three weight-loss steps for β-3 during the pyrolysis. Moreover, the microstructures of pyrolysis products obtained from β resins varied. The polarized microscopic images of β-1-P, β-2-P, and β-3-P showed a coarse fibrous structure, mosaic structure, and fine fibrous structure, respectively. The XRD and Raman spectroscopic analyses indicate that the content of well-ordered carbon structure in β-3-P was higher than those of the other two samples, and β-2-P has the highest level of amorphous carbon. This indicates that β-3-P has a good graphitizablity than the other two samples. This further proves that thermal treatment is a perfect method to produce a coal tar pitch-based carbon precursor with good graphitizablity, and air oxidation is an efficient method to produce an isotropic coal tar pitch-based carbon precursor.

Acknowledgements

This work was supported by the National Natural Science Foundation of China (U1361126), the Specialized Research Fund for the Doctoral Program of Higher Education (20132120110001).

References

1. E. Fitzer, K .H. KÖchling, H. Marsh, Recommended Terminology for the Description of Carbon as a Solid, *Pure Appl. Chem.*, **67**, 473 (1995).
2. G. Savage, *Carbon–Carbon Composites*, Chapman & Hall, London, UK, p. 156 (1992).
3. F. O. Oner, A. Yurum, Y. Yuruma, Structural Characterization of Semicokes Produced from the Pyrolysis of Petroleum Pitches, *J. Anal. Appl. Pyrol.*, **111**, 15 (2015).
4. B. Petrova, T. Budinova, E. Ekinci, N. Petrov, F. Yardim, Influence of Pitch Composition and Surface Properties of Petroleum Coke on Their Interaction During the Preparation of Carbon/Carbon Composites, *Carbon*, **45**, 704 (2007).
5. I. Mochida, C. H. Ku, Y. Korai, Anodic Performance and Insertion Mechanism of Hard Carbons Prepared from Synthetic Isotropic Pitches, *Carbon*, **39**, 399 (2001).
6. V. Liedke, K. J. Huttinger, Mesophase Pitches as Matrix Precursor of Carbon Fiber Reinforced Carbon: II Stabilization of Mesophase Pitch Matrix by Oxygen Treatment, *Carbon*, **34**, 1067 (1996).
7. L. M. Manocha, M. Patel, S.M. Manocha, Carbon/Carbon Composites with Heat-treated Pitches I. Effect of Treatment in Air on the Physical Characteristics of Coal Tar Pitches and the Carbon Matrix Derived Therefrom, *Carbon*, **39**, 663 (2001).
8. D. Mikociak, A. Magiera, G. Labojko, S. Blazewicz, Effect of Nanosilicon Carbide on the Carbonization Process of Coal Tar Pitch, *J. Anal. Appl. Pyrol.*, **107**, 191 (2014).
9. B. Petrova, T. Budinova, N. Petrov, M. F. Yardim, E. Ekinci, M. Razvigorova, Effect of Different Oxidation Treatments on the Chemical Structure and Properties of Commercial Coal Tar Pitch, *Carbon*, **43**, 261 (2005).
10. B. Rhee, E. Fitzer, M. Ileym, Entwicklung des Graphitierungsverfahrens, *High Press. High Temp.*, **8**, 307 (1997).
11. E. Fitzer, K. Mueller, W. Schaefer, in: P.L. Walker Jr. (Ed.), *Chemistry and Physics of Carbon*, vol. 7, Marcel Dekker, New York, p. 263 (1971).
12. A. Mianowski, S. Blazewicz, Z. Robak, Analysis of the Carbonization and Formation of Coal Tar Pitch Mesophase Under Dynamic Conditions, *Carbon*, **41**, 2413 (2003).
13. T. Metzinger, K. J. Huttinger, Investigation on the Cross-linking of Binder Pitch Matrix of

Carbon Bodies with Molecular Oxygen – Part I. Chemistry of Reaction Between Pitch and Oxygen, *Carbon*, **35**, 892 (1997).
14. A. Méndez, R. Santamaría, R. Menéndez, Influence of Granular Carbons on the Pyrolysis
15. Behaviour of Coal-tar Pitches, *J. Anal. Appl. Pyrol.*, **58**, 825 (2001).
16. Y. G. Wang, Y. C. Chang, S. Ishida, Y. Korai, I. Mochida, Stabilization and Carbonization Properties of Mesocarbon Microbeads (MCMB) Prepared from a Synthetic Naphthalene Isotropic Pitch, *Carbon*, **37**, 969 (1999).
17. J. AlcanÄiz-Monge, D. Cazorla-AmoroÂs, A. Linares-Solano, Characterisation of Coal Tar Pitches by Thermal Analysis, Infrared Spectroscopy and Solvent Fractionation, *Fuel*, **80**, 48 (2001).
18. V. G. Rocha, M. Granda, R. Santamaría, Pyrolysis Behaviour of Pitches Modified with Different Additives, *J. Anal. Appl. Pyrol.*, **73**, 276 (2005).
19. M. D. Guillén, M. J. Iglesias, A. Domínguez, C. G. Blanco, Fourier Transform Infrared Study of Coal Tar Pitches, *Fuel*, **74**, 1595 (1995).
20. Z. H. Qin, H. Chen, Y. J. Yan, C. S. Li, L. M. Rong, X. Q. Yang, FTIR Quantitative Analysis Upon Solubility of Carbon Disulfide/N-methyl-2-pyrrolidinone Mixed Solvent to Coal Petrographic Constituents, *Fuel Process. Technol.*, **133**, 14 (2015).
21. J. V. Ibarra, E. Munoz, R. Moliner, FTIR Study of the Evolution of Coal Structure During Coalification Process, *Org. Geochem.*, **24**, 725 (1996).
22. E. L. Fuller, N. R. Smyrl, R. L. Howell, C. S. Daw, Chemistry and Structure of Coals: Evaluation of Organic Structure by Computer Aided Diffuse Reflectance Infrared Spectroscopy, *Am. Chem. Soc. Div. Fuel Chem.*, **29**, 1 (1984).
23. J. V. Ibarra, R. Moliner, A. J. Bonet, FTIR Investigation on Char Formation During the Early Stages of Coal Pyrolysis, *Fuel*, **73**, 918 (1994).
24. S. H. Wang, P. R. Griffiths, Resolution Enhancement of Diffuse Reflectance IR Spectra of Coal by Fourier Self-deconvolution: 1. C-H Stretching and Bending Modes, *Fuel*, **64**, 229 (1985).
25. P. C. Painter, R. W. Snyder, M. Starsinic, M. M. Coleman, D. W. Kuehn, A. Davis, Concerning the Application of FTIR to the Study of Coal: A Critical Assessment of Band Assignments and the Application of Spectral Analysis Programs, *Appl. Spectrosc.*, **35**, 475 (1981).
26. J. Bermejo, R. Menéndez, A. Figueiras, M. Granda, The Role of Low-Molecular-Weight Components in the Pyrolysis of Pitches, *Fuel*, **74**, 1792 (1995).
27. M. D. Guillén, A. Dominguez, M. J. Iglesias, Analysis of Coal Tar Pitch: Relations Between Thermal Behaviour and Composition, *Fuel*, **75**, 1101 (1996).
28. P. C. Painter, M. M. Coleman, R. G. Jenkins, P. W. Whang, P. L. Walker, Fourier Transform Infrared Study of Mineral Matter in Coal. A Novel Method for Quantitative Mineralogical Analysis, *Fuel*, **57**, 337 (1978).
29. P. C. Painter, R. W. Snyder, J. Youtcheff, P. H. Given, H. Gong, N. Suhr, Analysis of Kaolinite in Coal by Infrared Spectroscopy, *Fuel*, **59**, 364 (1980).
30. R. Morga, I. Jolonek, K. Kruszewska, W. Szulik, Relationships Between Quality of Coals, Resulting Cokes, and Micro-Raman Spectral Characteristics of These Cokes, *Int. J. Coal Geol.*, **144**, 130 (2015).
31. A. Sadezky, H. Muckenhuber, H. Grothe, R. Niessner, U. PÖschl, Raman Microspectroscopy of Soot and Related Carbonaceous Materials: Spectral Analysis and Structural Information, *Carbon*, **43**, 1731 (2005).
32. R. Morga, Micro-Raman Spectroscopy of Carbonized Semifusinite and Fusinite, *Int. J. Coal Geol.*, **87**, 253 (2011).
33. O. Beyssac, B. Goffé, J. P. Petitet, E. igneux, M. Moreau, J. N. Rouzaud, On the Characterization of Disordered and Heterogeneous Carbonaceous Materials by Raman Spectroscopy, *Spectrochim. Acta A*, **59**, 2267 (2003).
34. R. B. Finkelman, F. L. Fiene, P. C. Painter, Determination of Kaolinite in Coal by Infrared Spectroscopy-A Comment, *Fuel*, **60**, 643 (1981).
35. J. Ibarra, E. Muñoz, R. Moliner, FTIR Study of the Evolution of Coal Structure During the Coalification Process, *Org. Geochem.*, **24**, 725 (1996).
36. B. Manoj, A. G. Kunjomana, Study of Stacking Structure of Amorphous Carbon by X-ray Diffraction Technique, *Int. J. Electrochem. Sci.*, **7**, 3127 (2012).